NeuroImage 162 (2017) 186–198

Contents lists available at ScienceDirect

NeuroImage

journal homepage: www.elsevier.com/locate/neuroimage

# Neural congruence between intertemporal and interpersonal self-control: Evidence from delay and social discounting

Paul F. Hill [a,*], Richard Yi [b], R. Nathan Spreng [c,d], Rachel A. Diana [a]

[a] Department of Psychology, Virginia Tech, Blacksburg, VA 24061, USA
[b] Department of Health Education and Behavior, University of Florida, Gainesville, FL 32611, USA
[c] Laboratory of Brain and Cognition, Montreal Neurological Institute, Department of Neurology and Neurosurgery, McGill University, Montreal, QC, H3A 2B4, Canada
[d] Human Neuroscience Institute, Department of Human Development, Cornell University, Ithaca, NY 14853, USA

ARTICLE INFO

*Keywords:*
Delay discounting
Social discounting
Self-control
Prefrontal cortex
Medial temporal lobes
Temporoparietal junction

ABSTRACT

Behavioral studies using delay and social discounting as indices of self-control and altruism, respectively, have revealed functional similarities between farsighted and social decisions. However, neural evidence for this functional link is lacking. Twenty-five young adults completed a delay and social discounting task during fMRI scanning. A spatiotemporal partial least squares analysis revealed that both forms of discounting were well characterized by a pattern of brain activity in areas comprising frontoparietal control, default, and mesolimbic reward networks. Both forms of discounting appear to draw on common neurocognitive mechanisms, regardless of whether choices involve intertemporal or interpersonal outcomes. We also observed neural profiles differentiating between high and low discounters. High discounters were well characterized by increased medial temporal lobe and limbic activity. In contrast, low discount rates were associated with activity in the medial prefrontal cortex and right temporoparietal junction. This pattern may reflect biological mechanisms underlying behavioral heterogeneity in discount rates.

## 1. Introduction

Delay discounting (DD) is the tendency to subjectively devalue future rewards in favor of immediate gratification and is a commonly used measure of behavioral self-control (Green and Myerson, 2004). There is substantial variability in discount rates (Odum, 2011; Peters & Buchel, 2011) and individual differences are predictive of a broad range of behaviors, including general intelligence (Shamosh et al., 2008), purpose in life (Burrow & Spreng, 2016) and physical health (Moffitt et al., 2011). Moreover, excessive rates of DD are characteristic of several maladaptive and pathological behaviors (Bickel et al., 2012a, b). Much like the intertemporal choices in DD, social reciprocity can be characterized as a conflict between the immediate sacrifices of generosity and the long-term benefits of social cooperation (Axelrod and Hamilton, 1981; Boyer, 2008; Rachlin, 2002). For example, in an iterative Prisoner's Dilemma game, cooperation among agents promotes greater *long-term* payoffs but requires an agent to forgo the best *immediate* outcome. In order to maximize outcomes for oneself an agent must override the impulse to defect in order to build and sustain a cooperative relationship with an opponent, which will ultimately benefit the self. Discounting of future outcomes has consistently been found to correlate with the number of defections an agent makes against a tit-for-tat strategy (Harris and Madden, 2002; Stephens et al., 2002; Yi et al., 2005). Reciprocal altruism may therefore reflect a specific form of self-control (Rachlin, 2002).

Altruism can be measured via social discounting (SD), the tendency to subjectively devalue altruistic outcomes for others as a function of the perceived social distance separating oneself from a beneficiary (Jones and Rachlin, 2006; Rachlin and Jones, 2007; Safin et al., 2013). Emerging behavioral evidence highlights similarities between DD and SD. Both forms of discounting are well characterized as a hyperbolic function of increasing temporal and social distance (Jones and Rachlin, 2006, 2009; Rachlin and Jones, 2007) and may rely on shared psychological processes (Charlton et al., 2013; Locey et al., 2011; Yi et al., 2012; Yi et al., 2011). However, despite behavioral evidence for the effect of social distance on altruistic preferences, the neural basis of this effect has not been the focus of extensive investigation. Moreover, the degree to which these two forms of discounting draw on common and/or dissociable neural mechanisms remains unknown.

Despite the extensive functional overlap between DD and SD, dissociations between these two forms of discounting have been reported. For

* Corresponding author.
*E-mail address:* pfhill@vt.edu (P.F. Hill).

http://dx.doi.org/10.1016/j.neuroimage.2017.08.071
Received 9 May 2017; Accepted 24 August 2017
Available online 4 September 2017

example, reward magnitudes differentially modulate discounting behavior, with participants generally becoming *more* self-controlled (DD) but *less* altruistic (SD) as potential reward amounts increase (Rachlin and Jones, 2007; Yi et al., 2012). Jones and Rachlin (2009) observed that, despite significant correlations between DD and SD, charitable contributions on a public-goods task positively covaried with altruistic preferences but not intertemporal self-control. Moreover, choices directly benefiting others tend to be more risk-adverse than decisions that only involve oneself, particularly when choices involve potential losses (for review, see Atanasov, 2016). Taken together, these behavioral findings suggest some qualitative differences between DD and SD.

DD is relatively well-characterized within the neuroimaging literature. Despite a diverse array of experimental paradigms and reward modalities, common patterns of cortical and subcortical activity have been reported in regions comprising default, frontoparietal control, and mesolimbic reward networks (Carter et al., 2010). One hypothesis is that DD emerges from the relative contributions of these functionally specialized systems (Bechara et al., 2005; McClure and Bickel, 2014; McClure et al., 2004). For example, the ventromedial prefrontal cortex (VMPFC) has been identified as a key region involved with representing and tracking subjective valuation signals which are modulated by competing neurobehavioral systems (Jimura et al., 2013; Kable and Glimcher, 2007; Montague et al., 2006). Activity in the default and frontoparietal control networks (particularly in the prefrontal cortex) is associated with more far-sighted decisions and higher rates of self-control (Benoit et al., 2011; Jimura et al., 2013; McClure et al., 2004; Peters and Buchel, 2010). The default network has been implicated in a number of diverse autobiographical processes, including the ability to vividly imagine or anticipate future events and outcomes (Andrews-Hanna et al., 2014a, b; Spreng et al., 2015), and is observed to flexibly couple with the frontoparietal control network during complex goal-directed planning (Gerlach et al., 2011; Spreng et al., 2010). Upregulation of the default network may reflect the ability to vividly anticipate future outcomes and therefore lead to increasing valuation signals in the VMPFC for time-delayed options (Benoit et al., 2011; Boyer, 2008; Hakimi and Hare, 2015; Peters and Buchel, 2010).

To date there has been only a single neuroimaging study investigating the neural basis of SD (Strombach et al., 2015). Similar to the extant literature on DD, SD was observed to result from a balance between selfish and generous motives encoded within valuation and default network regions, respectively. The VMPFC, in tracking the subjective value of rewards across time, may serve an analogous function within interpersonal contexts by tracking the long-term benefits of social cooperation (Montague et al., 2006; Rilling and Sanfey, 2011). Strombach and colleagues (2015) found modulations in VMPFC activity in response to subjective valuation signals associated with both selfish and generous choice options. Moreover, a psychophysiological interaction analysis revealed choice-dependent functional connectivity between the VMPFC and right temporoparietal junction (TPJ) during generous, but not selfish, choices. The TPJ is a node within the default network often observed in response to tasks involving social cognition (Andrews-Hanna et al., 2010; Andrews-Hanna et al., 2014a, b; Spreng et al., 2009). Thus, the existing evidence for the neural basis of SD indicates that, during prosocial choices, valuation signals in the VMPFC are modulated by superordinate prosocial preferences encoded in the TPJ (Strombach et al., 2015).

Despite behavioral evidence for similarities and dissociations between DD and SD, the neural basis of decisions regarding temporally and socially distal outcomes remains poorly understood. Behavioral similarities may suggest an underlying neural correspondence that, if identified, might reflect a "domain agnostic" network for deliberative decisions requiring intertemporal and interpersonal self-control. Alternatively, neural data may dissociate patterns of activity associated with discounting specificity. In the current study we used functional magnetic resonance imaging (fMRI) to scan participants as they completed both DD and SD tasks (see Bickel et al., 2009). FMRI data were analyzed using spatiotemporal partial least squares (PLS) in order to identify patterns of brain activity distinguishing between DD, SD, and control trials as well as patterns of brain activity covarying with behavioral measures of discounting.

## 2. Materials and methods

### 2.1. Participants

Twenty-six members of the Virginia Tech community (19 females, mean age = 24) were recruited to participate. All participants were right handed. One female participant was excluded from fMRI data analysis due to technological failures in stimulus presentation timing and syncing for a final N of 25.

### 2.2. Procedure

We incorporated the same task design and stimuli as a previous study investigating commonalities in the neural profiles underlying DD for real and hypothetical outcomes (Bickel et al., 2009) but extended the design to a SD task. Participants completed DD and SD trials for hypothetical monetary rewards during fMRI scanning. During DD trials, participants chose between receiving a variable outcome of less than $100 immediately or $100 in 1 week, 1 month, or 6 months. Immediate reward alternatives and presentation order were the same as those used in Bickel et al. (2009).

During SD trials, participants chose whether to forgo receiving a moderate outcome for themselves in lieu of allocating $100 to acquaintances at varying social distances. Before scanning, participants were prompted to imagine generating a list of the 100 people closest to them in the world where number 1 was their closest friend or relative and number 100 was a distant acquaintance (Jones and Rachlin, 2006; Rachlin and Jones, 2007). They were then asked to provide the first name and last initial of the persons occupying spots 1, 2, and 8 on this list. Using normative SD rates from prior studies (Jones and Rachlin, 2006; Rachlin and Jones, 2007), we selected social distances that would produce mean indifference points equivalent to those used to select the immediate reward alternatives for the DD task (Bickel et al., 2009). This ensured roughly equivalent percentage of smaller vs. larger reward selections across discounting trials. Participants were instructed that persons 1 and 2 were likely to be one's closest friends or relatives whereas person number 8 might be considered a good friend but outside of their inner circle. Participants were asked to abstain from listing financial benefactors (e.g., parents, grandparents) in order to avoid potential confounding effects of financial dependence on proximal social distances. Other biological relatives (e.g., siblings, cousins) were not excluded from this list. These names were then used as stimuli during the SD task. Participants also completed control trials in which they chose between two outcomes that did not include a temporal or social component (e.g. $64.27 or $100). Control trials required participants to assess the objective value of both outcomes but minimized the deliberative decision making requirements of DD and SD trials. We used a mixed block/event-related fMRI design divided into two functional runs counterbalanced across the two discounting conditions (Fig. 1). Each run included 56 trials (28 discounting trials and 28 control trials). Trials were separated within each block by a jittered fixation ITI (2–4s). Blocks of discounting and control trials were separated by a 12s fixation inter-block interval. Trial order and outcome magnitudes were matched across runs and were the same as in Bickel et al. (2009).

### 2.3. MRI data acquisition

MRI data were acquired at the Virginia Tech Carillion Research Institute Human Neuroimaging Lab using a 3 T Siemens Tim Trio scanner equipped with a 12-channel head coil. Prescreening interviews were conducted to ensure safety in the scanner, and headphones were

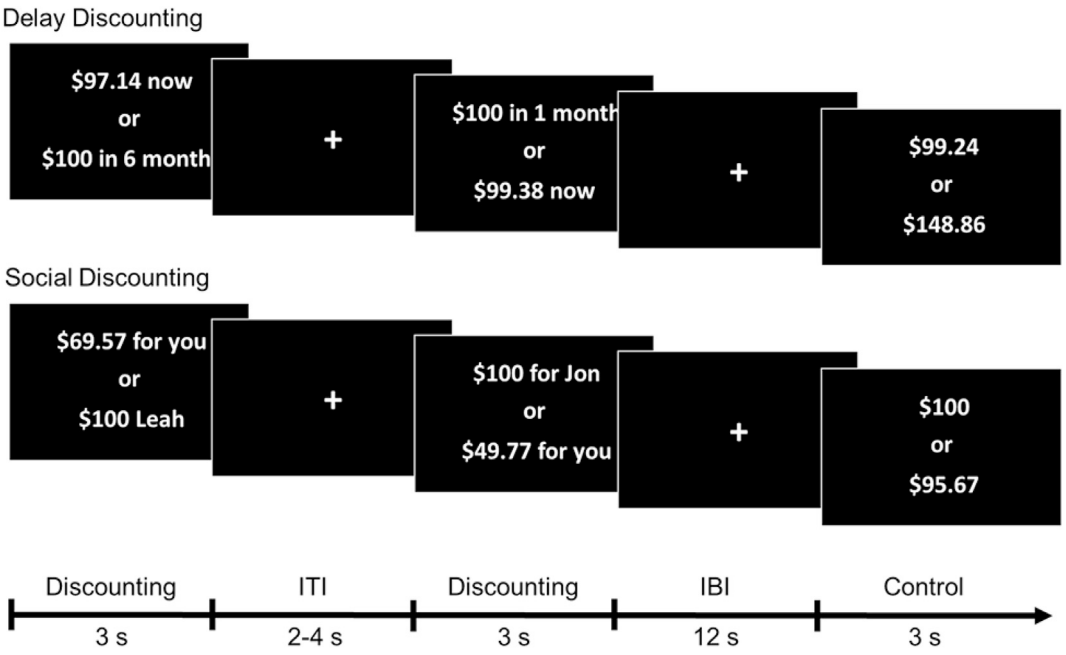


**Fig. 1. Task Design.** Participants completed a delay and social discounting task during fMRI scanning. During delay discounting trials, participants chose between receiving a variable outcome of less than $100 immediately vs. receiving $100 in 1 week, 1 month, or 6 months. During social discounting trials, participants chose between receiving a variable outcome of less than $100 for themselves vs. allocating $100 to beneficiaries of varying social distances (persons 1, 2, or 8 of 100). During control trials, participants chose between receiving two monetary amounts (e.g., $75 vs $30) with no temporal or social dimension. Control trials thus required participants to evaluate and compare the relative value of both options, but did not require deliberative decision making or evaluation of distance. ITI = Inter-trial interval, IBI = Inter-block interval.

provided to attenuate acoustic noise from the scanner. Padding and adjustable head restraints minimized head movement. Functional data collection consisted of a gradient echoplanar imaging (EPI) sequence (repetition time/TR = 2000 ms; echo time/TE = 23 ms; field of view = 220). Each volume included 40 slices with a thickness of 3.4 mm and no interslice gap. Voxel size for functional images was 3.4 × 3.4 × 3.4 mm. Each run included 300 EPI volumes with some participants' runs truncated to 294 vol due to a technical error. The first six runs were discarded to allow for equilibration effects. Anatomical images were collected using an MPRAGE sequence (voxel size = 0.9 × 0.9 × 0.9 mm).

### 2.4. Preprocessing and analysis

All imaging preprocessing was performed using Statistical Parametric Mapping (SPM8) software (Wellcome Trust Centre for Neuroimaging, London). EPI data were slice-time corrected with sinc interpolation to account for differences in the timing of adjacent slice acquisition. Then, the functional images for an individual participant were brought into spatial alignment by using a six-parameter, rigid-body transformation. Following realignment, the high-resolution MPRAGE structural image for each participant was co-registered to the mean EPI for each participant. Spatial normalization was conducted using a segmentation-based procedure. First, the unified segmentation tool in SPM8 was used to calculate normalization parameters based on each participant's co-registered high-resolution MPRAGE. These normalization parameters were then applied to the EPI images to transform them into Montreal Neurological Institute (MNI) template space. Finally, the images were spatially smoothed with an 8 mm full-width at half-maximum Gaussian filter.

Run order and motion parameter outliers were modeled as covariates of no interest. Motion parameter outliers were identified at the individual-subject level using the Artifact Detection Tools (http://gablab.mit.edu/index.php/software) in SPM8 with thresholds for global signal intensity (z = 5), translational movement (0.5 mm), and rotational movement (0.005 rad) with each outlier being modeled as an individual covariate of no interest.

#### 2.4.1. Spatiotemporal partial least squares

FMRI data were analyzed using spatiotemporal partial least squares (PLS; McIntosh and Lobaugh, 2004). Spatiotemporal PLS is a multivariate, data-driven technique that analyzes covariance between spatiotemporal patterns of whole brain activity and the experimental task design (mean-centered PLS) or a behavioral measure(s) of interest (behavioral PLS). This covariance is decomposed using singular value decomposition in order to identify orthogonal latent variables (LVs) that describe the optimal relationship between brain activity and cognitive tasks (mean-centered PLS) or between brain activity and behavioral performance (behavioral PLS). For the purposes of this study, we performed a mean-centered PLS in order to identify changes in mean brain activity in response to the onsets of the DD, SD, and Control tasks. An additional behavioral PLS analysis was performed to identify patterns of brain activity that capture individual differences in discounting behavior (i.e., choice indices) on the DD and SD tasks.

The statistical significance of each LV was determined using 500 permutation tests that randomly reordered and decomposed the data to calculate new sets of LVs. Each original LV was assigned a probability based on the number of times a statistic (i.e., amount of covariance explained or singular value) from the permuted data exceeded the original values. Each brain voxel was assigned a weighted salience value that was proportional to its covariance with the task design (or behavioral measure) at each TR of the pre-specified 14 *s* (7 TR) temporal window. The reliability of voxel saliences within a LV were determined using bootstrap resampling with replacement to estimate standard errors in 300 bootstrap samples. Unlike traditional univariate techniques, PLS is computed in a single analytic step, negating the need to correct for multiple comparisons. Clusters of 20 or more voxels in which the bootstrap-to-standard-error ratio (BSR) (similar to a z-score) was greater than 3 (approximate $p = 0.003$) are reported.

#### 2.4.2. General linear model (GLM) analyses

We performed a general linear model (GLM) analysis in order to identify dissociable patterns of brain activity associated with the DD and SD tasks compared to control. For each participant, the onset of each trial

was modeled with the canonical hemodynamic response function (HRF) with run order and movement parameters entered as nuisance regressors. Contrast images of DD and SD relative to control were generated and were then entered into a second level random effects analysis where they were directly contrasted with one another to identify regions preferentially associated by the DD and SD tasks, respectively. In a separate analysis, we submitted individual subject DD and SD contrast images to a second level random effects null conjunction analysis to determine areas of common brain activations in response to the DD and SD tasks (Price and Friston, 1997; Friston et al., 2005). Brain regions that survived a threshold of $p < 0.001$ uncorrected with a minimum of 10 contiguous voxels are reported in the text and tables below.

## 3. Results

### 3.1. Behavioral Results

Behavioral data were analyzed using RStudio 3.2.5 (RStudio Team, 2015). We calculated discounting parameters for each subject and condition to model the effects of temporal and social distance on behavioral preferences. The choice index was defined as the frequency of larger time-delayed options (DD trials) or larger altruistic options (SD trials) chosen vs. the total number of all options chosen for each discounting condition. This measure has been used to model the effects of temporal delay on choice preferences in previous neuroimaging studies using task designs that do not allow for robust estimation of hyperbolic discount rates, as was the case in this study (Benoit et al., 2011; Boettiger et al., 2007; Mitchell, Fields, D'Esposito and Boettiger, 2005). Participants chose the larger amount on 99.6% of control trials indicating successful conformity with task instructions and a lack of deliberative decision making in the absence of temporal or social delays. Control trials are not included in any of the subsequent behavioral analysis reports.

Composite choice index scores collapsed across distance were logit transformed in order to ensure parametric validity (Warton and Hui, 2011) and then compared across the two discounting conditions using a two-tailed paired samples *t*-test. As seen in Fig. 2A, participants were generally less likely to select the larger delayed reward during DD trials than they were to select the larger altruistic reward during SD trials, though this difference was not statistically significant ($t_{(24)} = -1.93$, $p = 0.065$). A one-way analysis of variance (ANOVA) revealed a significant main effect of condition (DD, SD, and Control) on choice reaction time (RT) ($F_{(2,\ 2\ 770)} = 844$, $p < 0.001$). Post-hoc Tukey HSD pairwise comparisons indicated that choice RT on DD ($M = 2048.5$ ms, $SD = 564.03$ ms) and SD ($M = 2012.7$ ms, $SD = 604.93$ ms) trials were significantly longer than control ($M = 1\ 271.2$ ms, $SD = 365.40$ ms) trials ($p < 0.001$). Response latencies on the DD and SD tasks were not significantly different ($p = 0.361$).

Composite choice index scores were not significantly correlated between DD and SD conditions ($r_{(23)} = -0.26$, $p = 0.216$) indicating that, within our sample, impulsive individuals were not necessarily selfish (Fig. 2B). We did note one value that appeared to be an outlier (DD = 1); however, omitting this value did not change the significance of this correlation ($r_{(22)} = 0.06$, $p = 0.792$). The restricted range of temporal and social delays used in this study may have prevented us from identifying a robust relationship between discount rates. Despite evidence that temporal and social distance are represented along a common dimension of psychological distance (Trope and Liberman, 2010), there may be idiosyncratic factors that influence intra-individual perceptions of temporal and social distance that were not captured in our behavioral data (e.g., personal goals or geographic proximity).

### 3.2. fMRI results

#### 3.2.1. Mean-centered PLS of discounting and control trials

The mean-centered PLS analysis of discounting and control trials identified one significant latent variable (i.e., LV1) reflecting a pattern of brain activity that differentiated the two discounting tasks from the control condition ($p = 0.002$; 76.03% covariance explained; Fig. 3). DD and SD covaried together and engaged a widespread pattern of brain activity in areas that are consistent with previous fMRI studies of DD (Carter et al., 2010) including the medial prefrontal cortex, lateral orbitofrontal cortex, anterior cingulate, bilateral dorsolateral prefrontal cortex (DLPFC), bilateral middle temporal gyri, posterior cingulate, precuneus, bilateral posterior parietal cortex, ventral striatum, and anterior insula (Table 1A). The areas of DD-SD overlap revealed by LV1 largely correspond to areas comprising default (Spreng et al., 2009), cognitive control (Vincent et al., 2008), and valuation networks

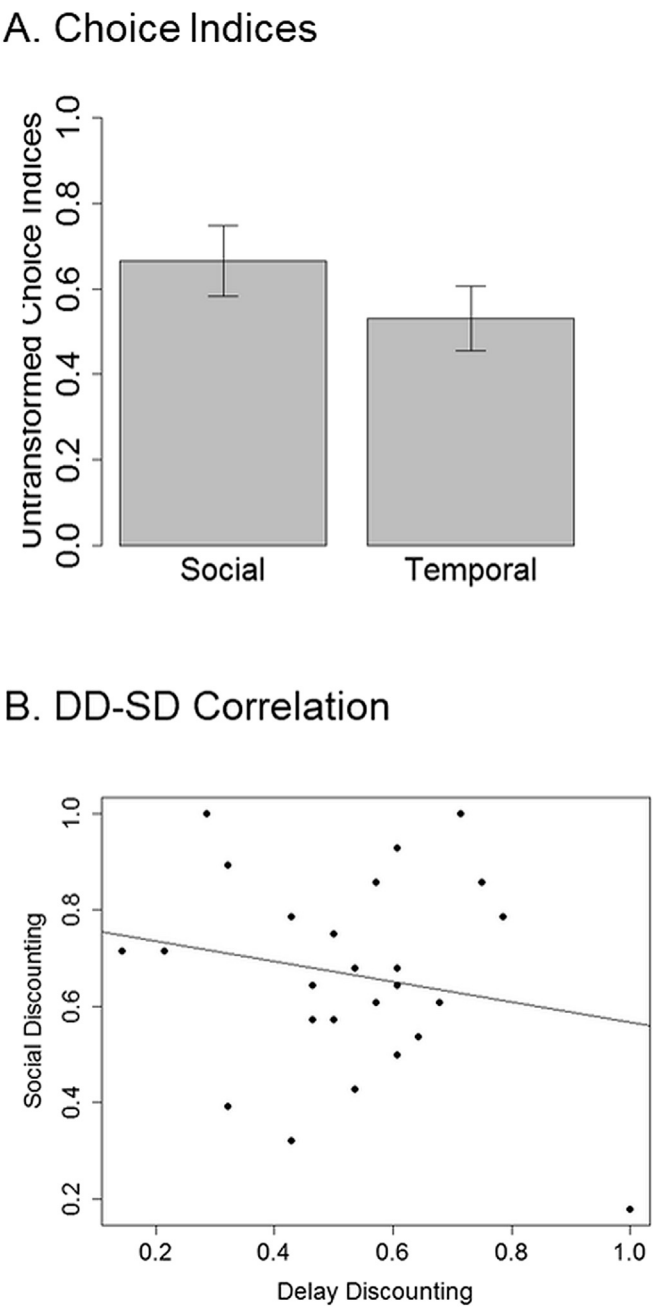


**Fig. 2. Behavioral Results.** (A) Bar plots of untransformed choice indices indicate that participants were generally more likely to select the altruistic option during SD trials than they were to select the far-sighted option during DD trials, though this differences was not statistically significant. Error bars represent standard error. (B) A scatter plot of DD and SD choice indices. DD and SD choice indices were not significantly correlated. Note that behavioral analyses were performed on logit transformed values. Untransformed values are presented here for ease of interpretation.

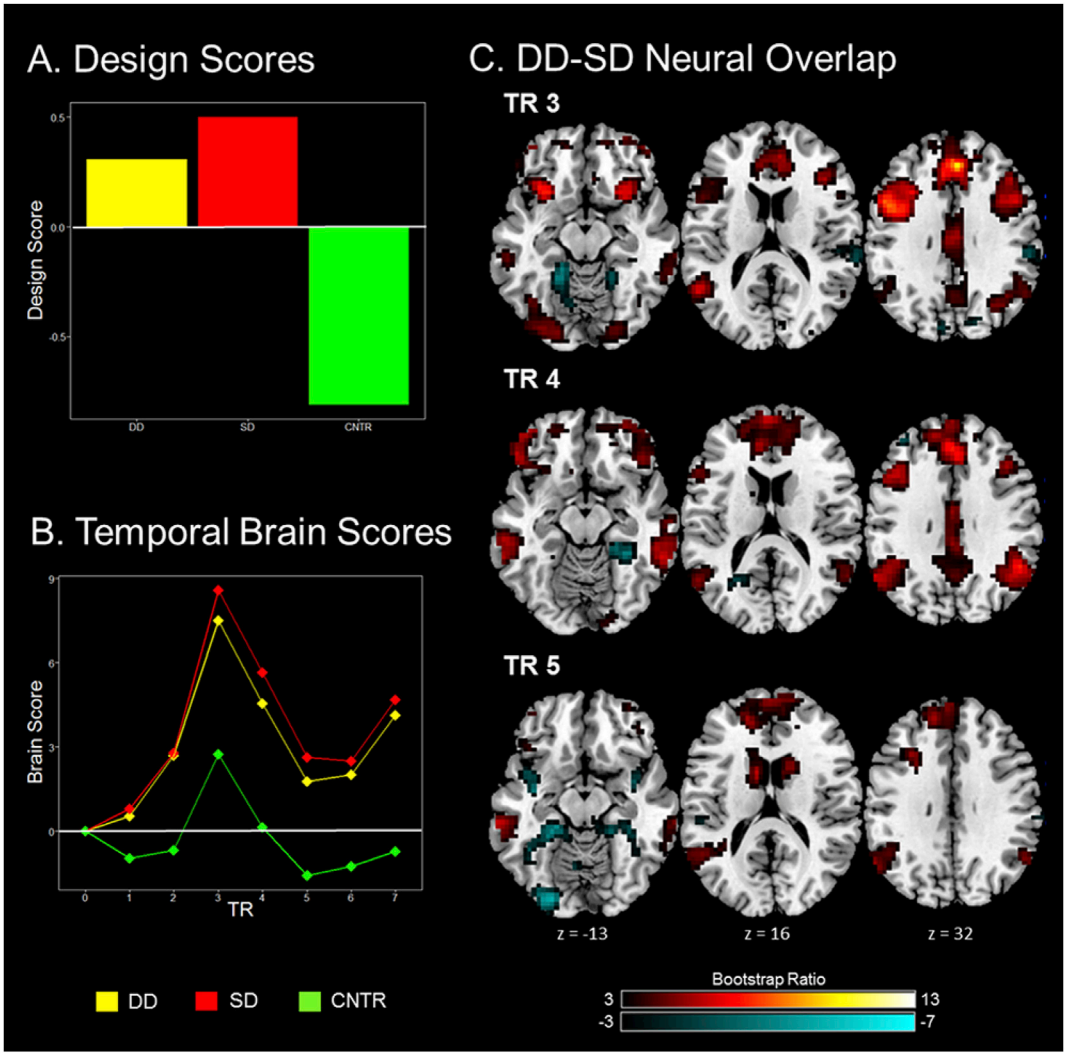


**Fig. 3. Mean-Centered PLS.** A mean-centered PLS identified a pattern of brain activity that differentiated the two discounting tasks from the control condition. (A) A plot of design scores indicating the correlation between each task and corresponding pattern of brain activity. These design scores reveal overlap between the DD and SD tasks and differentiate the two discounting tasks from control trials. (B) Weighted average of brain activation across all voxels during a 14s temporal window (divided into 2s TRs) following trial onset. This plot reveals greater activity during the DD and SD tasks compared to control trials which peaked during the 3rd TR. This plot also reveals temporal covariance between whole brain activity in response to the DD and SD tasks. (C). Brain regions in which activation was associated with the two discounting tasks (warm colors) and control trials (cyan) are shown for TRs 3–5. Areas shown were thresholded at $p = 0.003$ with a minimum of 20 contiguous voxels.

(Montague et al., 2006), reflecting recruitment of common component processes during both forms of discounting. In contrast, the patterns of neural activity associated with the control task identified in LV1 included bilateral activations in dorsal anterior cingulate, posterior insula (extending into amygdala), secondary somatosensory cortex, fusiform gyrus, parahippocampal cortex (extending into posterior visual association areas), left DLPFC, and middle cingulate (Table 1B). A second mean centered PLS analysis which compared patterns of brain activity associated with systematic and nonsystematic discount rates did not indicate any differences between the two groups on any of the tasks (Supplementary Materials, Figure S1).

We hypothesized that in addition to neural overlap, the DD and SD tasks would also evoke dissociable patterns of brain activity; however, the mean-centered PLS analysis did not reveal any significant patterns differentiating between the two discounting conditions. To explore this further, we ran a non-rotated PLS analysis which allowed for the specification of an a priori contrast between DD and SD trials. Even with the pre-existing bias to expect a dissociation of the two tasks, the analysis did not reveal any patterns of significant brain activity differentiating between DD and SD ($p = 0.371$).

### 3.2.2. *Univariate GLM analyses*

A second level random effects contrast of the single subject DD and SD contrast images identified brain areas that were preferentially active during the DD and SD tasks, respectively (Table 2). This analysis revealed unique activity in regions corresponding to self-appraisal and mentalizing subsystems of the default network (Andrews-Hanna et al., 2010; 2014a, b) during the SD task, including the medial prefrontal cortex, precuneus, posterior cingulate, and bilateral TPJ (Fig. 4A). The DD task was associated with increased activity in a small cluster of voxels centered in the left precentral gyrus extending into posterior insula; however, this cluster did not survive more conservative clusterwise corrections.

A conjunction analysis of individual subject DD and SD contrasts identified a pattern of brain activity which was largely consistent with areas identified by LV1 of the mean centered PLS analysis. This included increased brain activity in default (medial prefrontal cortex, posterior cingulate, precuneus, and bilateral middle temporal gyri), frontoparietal control (DLPFC, posterior parietal cortex) and mesolimbic reward (lateral orbitofrontal cortex, ventral striatum, and anterior insula) networks in response to the DD and SD tasks compared to control (Fig. 4B).

**Table 1A**
Regions covarying with discounting trials.

| Brain Region | MNI | | | BSR | Brain Region | MNI | | | BSR |
|---|---|---|---|---|---|---|---|---|---|
| | x | y | z | | | x | y | z | |
| **TR 1** | | | | | **TR 5 (cont)** | | | | |
| L. MTG | −54 | −37 | 0 | 4.503 | L. MTG | −65 | −31 | −14 | 5.839 |
| **TR 2** | | | | | L. Caudate Nucleus | −10 | 7 | 17 | 5.695 |
| L. Precentral Gyrus | −37 | 7 | 31 | 6.853 | R. Caudate Nucleus | 17 | 10 | 17 | 4.764 |
| L. MTG | −54 | −51 | 14 | 6.091 | R. Inferior Frontal Gyrus | 41 | 41 | −17 | 4.486 |
| R. Middle Cingulate | 7 | 17 | 44 | 5.739 | L. Inferior Frontal Gyrus | −51 | 31 | −7 | 4.476 |
| R. Inferior Frontal Gyrus | 34 | 14 | 24 | 5.427 | R. Orbitofrontal Cortex | 14 | 31 | 0 | 4.179 |
| R. Lingual Gyrus | 24 | −88 | −7 | 4.855 | L. Middle Frontal Gyrus | −37 | 10 | 51 | 3.950 |
| L. Insula | −31 | 20 | −7 | 4.439 | L. Mid Orbital Gyrus | −10 | 27 | −10 | 3.908 |
| R. Angular Gyrus | 54 | −58 | 37 | 4.244 | R. Mid Orbital Gyrus | 34 | 54 | −14 | 3.670 |
| R. Rectal Gyrus | 3 | 31 | −20 | 4.211 | **TR 6** | | | | |
| L. Inferior Occipital Gyrus | −31 | −82 | −10 | 4.020 | L. MTG | −51 | −37 | −3 | 6.590 |
| L. Precuneus | −3 | −54 | 34 | 3.933 | L. Inferior Frontal Gyrus | −34 | 10 | 27 | 5.849 |
| L. Middle Occipital Gyrus | −17 | −99 | 3 | 3.859 | R. Inferior Temporal Gyrus | 65 | −44 | −10 | 5.080 |
| **TR 3** | | | | | R. Inferior Frontal Gyrus | 41 | 37 | −17 | 4.938 |
| L. Superior Medial Gyrus | 3 | 37 | 34 | 13..021 | Left Inferior Frontal Gyrus | −44 | 31 | −17 | 4.929 |
| R. Lingual Gyrus | 24 | −88 | −10 | 7.468 | L. Superior Medial Gyrus | 0 | 27 | 58 | 4.815 |
| R. Angular Gyrus | 34 | −58 | 44 | 7.179 | Medial Prefrontal Cortex | −17 | 44 | 20 | 4.689 |
| L. Inferior Occipital Gyrus | −41 | −82 | −7 | 7.046 | R. Caudate Nucleus | 14 | 14 | 17 | 4.208 |
| L. MTG | −54 | −54 | 14 | 6.879 | R. Inferior Frontal Gyrus | 37 | 20 | 20 | 4.184 |
| R. Middle Orbital Gyrus | 37 | 58 | −3 | 6.299 | L. Caudate Nucleus | −14 | 14 | 7 | 3.984 |
| R. Inferior Temporal Gyrus | 65 | −44 | −10 | 5.017 | R. Caudate Nucleus | 20 | 34 | 0 | 3.949 |
| R. Rectal Gyrus | 3 | 27 | −24 | 3.983 | L. Caudate Nucleus | −20 | 27 | −7 | 3.798 |
| R. Fusiform Gyrus | 37 | −48 | −20 | 3.895 | L. Inferior Parietal Lobule | −41 | −61 | 54 | 3.606 |
| **TR 4** | | | | | **TR 7** | | | | |
| L. Superior Medial Gyrus | −3 | 37 | 37 | 9.600 | L. MTG | −54 | −34 | −14 | 5.692 |
| R. Angular Gyrus | 41 | −68 | 48 | 9.086 | L. Superior Medial Gyrus | −3 | 37 | 37 | 5.571 |
| L. Angular Gyrus | −48 | −61 | 44 | 8.249 | R. Middle Orbital Gyrus | 31 | 58 | −14 | 5.364 |
| R. Inferior Temporal Gyrus | 58 | −44 | −10 | 7.193 | R. Inferior Parietal Lobule | 48 | −44 | 51 | 5.032 |
| R. Inferior Frontal Gyrus | 44 | 31 | −17 | 5.269 | R. MTG | 61 | −44 | −7 | 4.920 |
| R. Premotor ctx | 14 | −24 | 58 | 4.813 | R. Middle Orbital Gyrus | 31 | 44 | −17 | 4.431 |
| R. Cerebellum | 41 | −65 | −24 | 4.289 | L. Anterior Insula | −24 | 24 | −3 | 4.334 |
| R. Lingual Gyrus | 14 | −95 | −14 | 3.647 | L. Middle Orbital Gyrus | −34 | 58 | −7 | 4.322 |
| **TR 5** | | | | | L. MTG | −54 | −58 | 20 | 3.978 |
| R. Inferior Parietal Lobule | 54 | −61 | 41 | 6.150 | L. Inferior Frontal Gyrus | −58 | 20 | 0 | 3.886 |
| L. Superior Medial Gyrus | 0 | 48 | 44 | 6.142 | L. Inferior Temporal Gyrus | −61 | −24 | −24 | 3.699 |
| R. MTG | 65 | −44 | −7 | 6.141 | | | | | |

Note: All activations survived a threshold of $p < 0.003$ (BSR $\geq 3$) with a minimum cluster size of 20 contiguous voxels. TR = time to repetition, BSR = Bootstrap Ratio, L = Left, R = Right, MTG = Middle Temporal Gyrus.

Direct contrasts of non-discounted vs. discounted trials on the DD and SD tasks identified considerably less brain activity than compared to control. Non-discounted trials on the DD task were associated with significantly greater bilateral activity in the precuneus than discounted trials. On the SD task, non-discounted trials were associated with increased activity in several small clusters located in right lateralized

**Table 1B**
Regions covarying with control trials.

| Brain Region | MNI Coordinates | | | BSR | Brain Region | MNI Coordinates | | | BSR |
|---|---|---|---|---|---|---|---|---|---|
| | x | y | z | | | x | y | z | |
| **TR 1** | | | | | **TR 4** | | | | |
| L. Cerebellum | −17 | −65 | −24 | −6.130 | L. Middle Frontal Gyrus | −34 | 41 | 37 | −7.449 |
| L. Lingual Gyrus | 0 | −82 | 3 | −5.138 | R. Fusiform Gyrus | 34 | −41 | −10 | −5.389 |
| L. Lingual Gyrus | −27 | −88 | −14 | −5.107 | L. Retrosplenial ctx | −27 | −54 | 0 | −5.141 |
| L. Parahippocampal ctx | −17 | −31 | −14 | −5.053 | L. Calcarine Gyrus | −24 | −61 | 17 | −4.062 |
| R. Medial Temporal Pole | 44 | 17 | −31 | −4.915 | **TR 5** | | | | |
| L. Superior Temporal Gyrus | −54 | −14 | 10 | −4.405 | L. Middle Occipital Gyrus | −17 | −95 | −3 | −10.475 |
| **TR 2** | | | | | R. Calcarine Gyrus | 20 | −95 | −3 | −8.351 |
| L. Supramarginal Gyrus | 54 | −27 | 27 | −8.083 | L. Parahippocampal ctx | −20 | −34 | −14 | −5.157 |
| R. Cerebellum | 17 | −37 | −17 | −6.254 | R. Amygdala | 37 | 0 | −17 | −4.835 |
| L. Superior Temporal Gyrus | −54 | −7 | 3 | −5.771 | L. Insula | −37 | −7 | −14 | −4.819 |
| L. Superior Parietal Lobule | −20 | −51 | 65 | −5.705 | R. Cerebellum | 17 | −34 | −17 | −4.672 |
| L. MTG | −48 | −68 | 0 | −4.314 | L. Cerebellum | −7 | −65 | −17 | −4.645 |
| **TR 3** | | | | | L. Precentral Gyrus | −14 | −7 | 68 | −3.885 |
| R. Superior Temporal Gyrus | 68 | −31 | 10 | −5.826 | R. SupraMarginal Gyrus | 65 | −27 | 31 | −3.546 |
| R. Parahippocampal ctx | 27 | 3 | −34 | −5.671 | **TR 6** | | | | |
| L. Parahippocampal ctx | −31 | −44 | −7 | −5.469 | R. Calcarine Gyrus | 20 | −99 | 3 | −5.677 |
| R. Lingual Gyrus | 20 | −48 | −10 | −5.005 | L. Fusiform Gyrus | −17 | −37 | −14 | −4.779 |
| R. Cuneus | 14 | −82 | 24 | −4.969 | | | | | |
| L. Cuneus | −10 | −85 | 31 | −3.923 | | | | | |

Note: All activations survived a threshold of $p < 0.003$ (BSR $\leq -3$) with a minimum cluster size of 20 contiguous voxels. TR = time to repetition, BSR = Bootstrap Ratio, L = Left, R = Right, MTG = Middle Temporal Gyrus.

**Table 2**
GLM peak coordinates.

| Brain Region | MNI Coordinates | | | *t*-score | Cluster size (voxels) | FDR |
|---|---|---|---|---|---|---|
| | x | y | z | | | |
| **Social > Delay** | | | | | | |
| L. Precuneus | 0 | −61 | 32 | 6.8 | 414 | 0.001 |
| R. Precuneus | 10 | −54 | 32 | 5.73 | | |
| L. Superior Medial Gyrus | −7 | 55 | 25 | 5.4 | 441 | 0.001 |
| R. Anterior Cingulate | 4 | 51 | 18 | 4.98 | | |
| R. VMPFC | 4 | 55 | −13 | 4.81 | | |
| L. Middle Temporal Gyrus | −44 | −61 | 21 | 5.2 | 80 | 0.008 |
| L. Middle Temporal Gyrus | −54 | −17 | −13 | 5 | 73 | 0.011 |
| L. Middle Temporal Gyrus | −47 | −24 | −9 | 4.18 | | |
| R. Angular Gyrus | 48 | −54 | 25 | 4.86 | 99 | 0.004 |
| R. Middle Temporal Gyrus | 55 | −64 | 18 | 3.35 | | |
| **Delay > Social** | | | | | | |
| L. Precentral Gyrus | −41 | 4 | 18 | 3.64 | 12 | 0.257 |
| L. Insula | −34 | −3 | 18 | 3.61 | | |
| **Social + Delay Conjunction** | | | | | | |
| L. Middle Occipital Gyrus | −17 | −98 | 4 | 9.41 | 1 134 | 0.001 |
| R. Calcarine Gyrus | 17 | −98 | 4 | 7.35 | | |
| L. Fusiform Gyrus | −37 | −68 | −13 | 6.25 | | |
| R. Inferior Parietal Lobule | 44 | −54 | 45 | 8.31 | 560 | 0.001 |
| R. Angular Gyrus | 38 | −61 | 52 | 7.73 | | |
| R. Precuneus | 7 | −68 | 45 | 4.21 | | |
| L. Superior Medial Gyrus | −7 | 34 | 32 | 8.13 | 2 552 | 0.001 |
| R. Middle Frontal Gyrus | 31 | 17 | 55 | 7.74 | | |
| L. Middle Frontal Gyrus | −41 | 4 | 55 | 7.7 | | |
| L. Angular Gyrus | −37 | −58 | 42 | 7.52 | 449 | 0.001 |
| R. Inferior Frontal Gyrus | 31 | 24 | −6 | 6.61 | 90 | 0.008 |
| L. Middle Temporal Gyrus | −51 | −41 | 4 | 5.61 | 148 | 0.001 |
| L. Inferior Temporal Gyrus | −61 | −27 | −19 | 4.99 | | |
| L. Middle Temporal Gyrus | −58 | −41 | −13 | 4.6 | | |
| R. Caudate Nucleus | 10 | 10 | 11 | 5.41 | 54 | 0.027 |
| R. Thalamus | 10 | −10 | 11 | 4.11 | | |
| R. Middle Temporal Gyrus | 58 | −37 | −13 | 5.28 | 104 | 0.005 |
| R. Inferior Temporal Gyrus | 61 | −17 | −23 | 5.14 | | |
| R. Posterior Cingulate | 4 | −30 | 32 | 4.39 | 64 | 0.020 |
| R. Middle Cingulate | 0 | −3 | 28 | 3.68 | | |
| L. Caudate Nucleus | −13 | −7 | 15 | 4.27 | 42 | 0.044 |
| L. Caudate Nucleus | −13 | 7 | 11 | 4.16 | | |
| **DD discounted > DD non-discounted** | | | | | | |
| *no suprathreshold clusters* | | | | | | |
| **SD discounted > SD non-discounted** | | | | | | |
| *no suprathreshold clusters* | | | | | | |
| **DD non-discounted > DD discounted** | | | | | | |
| L. Precuneus | −10 | −68 | 35 | 4.61 | 70 | 0.047 |
| R. Precuneus | 14 | −64 | 35 | 4.18 | | |
| **SD non-discounted > SD discounted** | | | | | | |
| R. Anterior Insula | 41 | 7 | 4 | 4.09 | 15 | 0.759 |
| R. Amygdala | 31 | 7 | −23 | 4.06 | 12 | 0.759 |
| L. Precuneus | −13 | −44 | 62 | 3.78 | 15 | 0.759 |
| R. Precentral Gyrus | 14 | −24 | 72 | 3.57 | 17 | 0.759 |

Note: All activations survived a threshold of $p < 0.001$ uncorrected with a minimum cluster size of 10 contiguous voxels. L = Left, R = Right, FDR = Clusterwise False Discovery Rate.

anterior insula, amygdala, precentral gyrus, and left somatosensory cortex as compared to discounted trials; however, none of these clusters survived the clusterwise correction. Reverse contrasts did not reveal any increased brain activity in response to discounted compared to non-discounted trials for either of the discounting tasks. Finally, a contrast between non-discounted and discounted trials, collapsed across tasks, did not reveal any suprathreshold clusters.

### 3.2.3. *Behavioral PLS of choice index during discounting trials*

We performed a behavioral PLS analysis to assess the relationship between brain activity and behavioral discounting performance (i.e., choice indices). This analysis identified a single significant LV that jointly captured individual differences on the DD and SD tasks ($p = 0.040$; 60.51% covariance explained). This LV corresponded with a pattern of brain activity that covaried with DD ($r = 0.75$) and SD ($r = 0.70$) discount rates (Fig. 5).

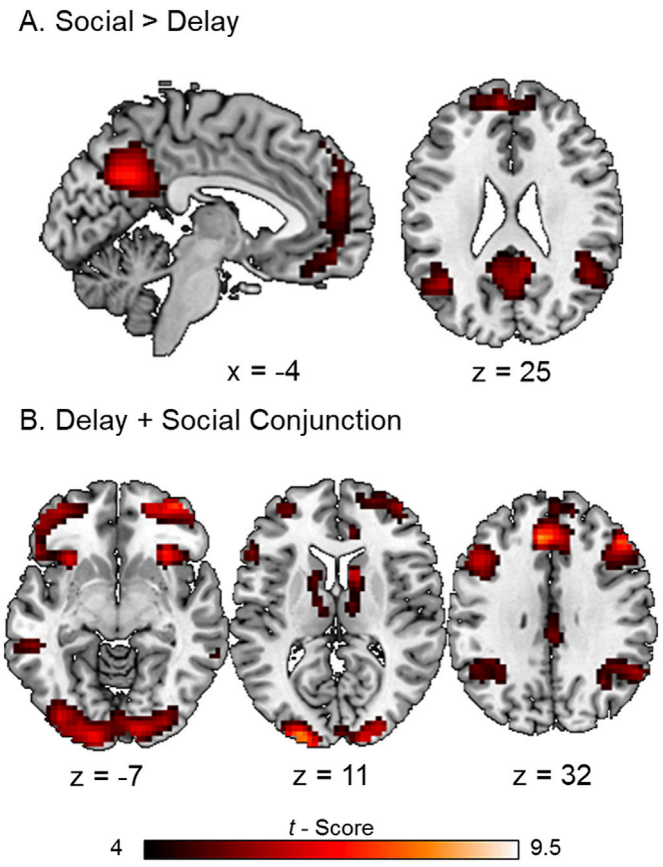


**Fig. 4. Univariate GLM Results.** (A) Areas of the default network were preferentially active in response to the SD task compared to DD. (B) A null conjunction analysis revealed areas of common brain activations in response to the DD and SD tasks. Areas shown survived a threshold of $p < 0.001$ uncorrected with a minimum of 10 contiguous voxels.

Activity in bilateral medial temporal lobes (MTL) was negatively modulated by choice indices across both discounting conditions (Fig. 5A top panel). That is, higher rates of impulsivity and/or selfishness (indicated by lower DD and SD choice index scores, respectively) were associated with increased MTL activity. We observed a similar negative relationship between choice indices and bilateral activity in the fronto-insular salience network (Fig. 5A bottom panel) involved with regulating bottom-up attention towards environmental stimuli (Sridharan et al., 2008) as well as mesolimbic areas such as left ventral striatum and bilateral amygdala. Additional areas exhibiting greater activity among high discounters are presented in Table 3A. The behavioral PLS also revealed a positive relationship between DD and SD choice indices and activity in the VMPFC and right TPJ (Fig. 5B) indicating greater activity among these regions in response to higher rates of self-control and/or altruism. Additional areas exhibiting greater activity among low discounters are presented in Table 3B

## 4. Discussion

Much like behavioral self-control, altruism can be characterized as a conflict between the immediate sacrifices of generosity and the long-term benefits of social cooperation. Altruism may therefore reflect a specific

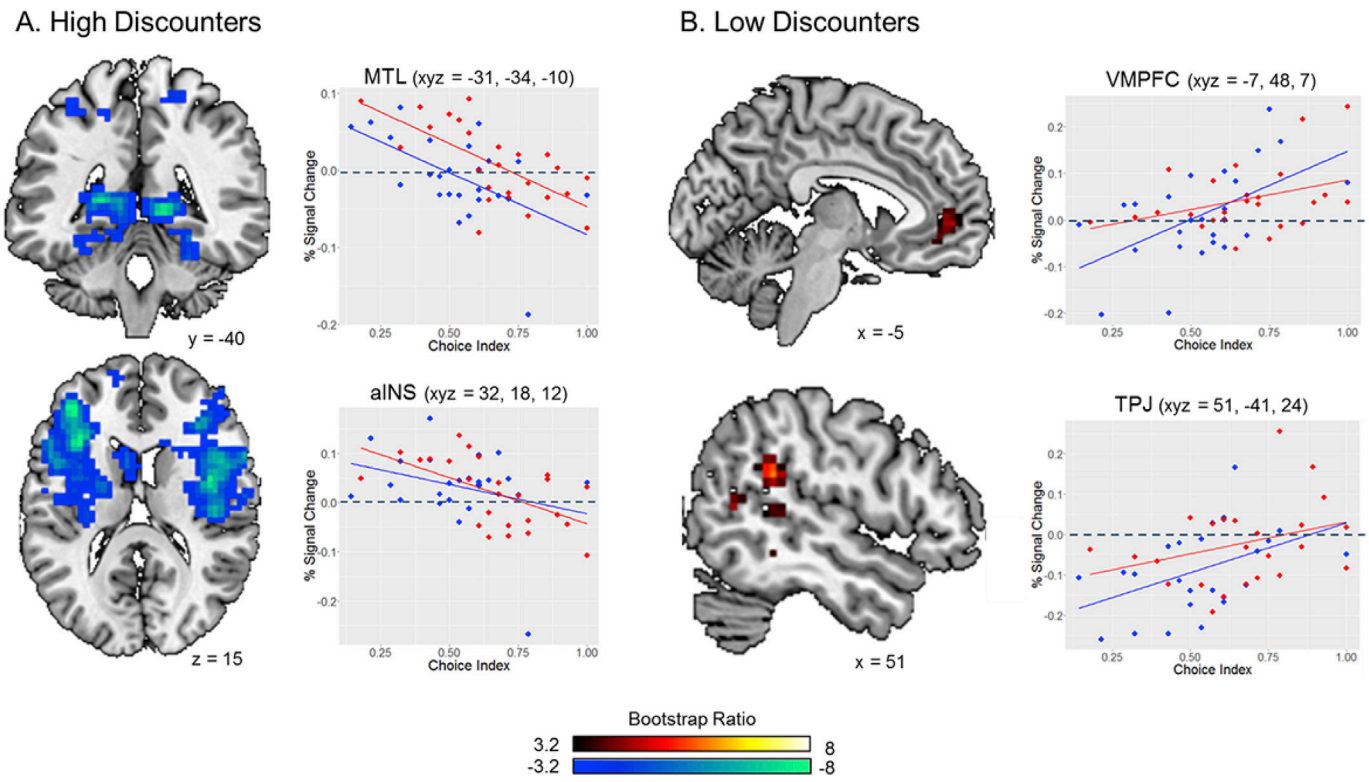


**Fig. 5. Behavioral PLS.** A behavioral PLS of choice index scores identified patterns of brain activity that jointly covaried with DD and SD choice indices and differentiated between high and low discounters. (A) High rates of DD and SD (cool colors) were associated with increased bilateral MTL and limbic activity. Choice indices were negatively correlated with bilateral MTL and anterior insula activity (peak correlation 7–8 s following trial onset). (B) Low rates of DD and SD (warm colors) were associated with increased activity in the ventromedial prefrontal cortex and less *deactivation* in the right temporoparietal junction. Positive correlations between choice indices and activity in the ventromedial prefrontal cortex and right temporoparietal junction peaked 3–4 s following trial onset. Peak correlations between mean brain activity and behavioral discount rates occurred between TRs 2–4. Images displayed in this figure indicate neural responses that are most consistent with our predictions and correspond to TRs 4 (A) and 2 (B). See Figure S2 in Supplemental Materials for a temporal unfolding of brain-behavior covariance. Scatter plots: blue = DD, red = SD.

form of self-control. Using DD and SD as behavioral indices of self-control and altruism, respectively, researchers have identified a close behavioral correspondence between decision making processes that support choices involving future and other-regarding outcomes. However, despite this extensive functional overlap, discrepancies between these two forms of discounting are also observed. Here, we demonstrate that DD and SD draw from highly overlapping brain regions. Our results provide evidence for a core domain general network supporting deliberative intertemporal and interpersonal self-control.

These results are particularly critical in light of the social influences and consequences of excessive impulsivity. Excessive DD is characteristic of a range of maladaptive behaviors and psychiatric conditions that beget negative social consequences (e.g., addiction, problem gambling, risky sexual practices) (Bickel et al., 2012a, b). There is also growing evidence for the influence of social context on economic decisions and impulsivity (Bickel et al., 2012a, b; Charlton et al., 2013; Kishida and Montague, 2012). For example, using a social delay discounting task, Charlton et al. (2013) observed that individuals discount less when the outcome of their choice is shared by a group ("we now" vs. "we later") vs. choices involving an individual outcome ("me now" vs. "me later") which the authors suggest may reflect the additive influence of temporal and social distance. A similar effect was observed to distinguish between different substance using populations (Bickel et al., 2012a, b). Hazardous-to-harmful drinkers were observed to discount more for individual outcomes (i.e., higher delay discounting) than non-problem drinkers; however, this effect disappeared when intertemporal outcomes were divided equally among members of a group. A similar effect was not observed among smokers, who demonstrated higher rates of discounting across both individual and social contexts. The authors speculate that this pattern of results may reflect the sociality of drinking and the growing restrictions of smoking in social contexts, respectively (Bickel et al., 2012a, b).

### 4.1. Regions of DD-SD overlap

We observed extensive neural overlap during both forms of discounting in regions comprising a number of functionally specialized brain networks. This finding was consistent across PLS and GLM-based analytical approaches. Regions of neural overlap closely resembled patterns commonly reported in neuroimaging studies of DD, suggesting that both forms of decision making may draw from a core set of component neurocognitive processes regardless of whether the decision involves intertemporal or interpersonal outcomes. We observed common patterns of bilateral brain activity in frontoparietal control regions involved with behavioral inhibition and cognitive control, including the anterior cingulate, DLPFC, posterior parietal cortex, and anterior insula. These results are consistent with the act of discounting requiring deliberative choices between competing options, thereby recruiting similar executive processes.

We also observed neural overlap in regions comprising the default network, including medial prefrontal cortex, bilateral medial temporal gyri, posterior cingulate and precuneus. Envisioning the future and simulating the viewpoints and actions of others are among the diverse autobiographical behaviors supported by the default network (Andrews-Hanna et al., 2014a, b). Choices involving future and social outcomes may draw on the prospective and social cognitive processes supported by the default network, respectively. The default network has been observed to interact with the frontoparietal control network in support of goal-directed autobiographical planning (Gerlach et al., 2011, 2013; Spreng et al., 2010) and discordance between these two networks is associated

**Table 3A**
Regions associated with high rates of discounting.

| Brain Region | MNI Coordinates | | | BSR | Brain Region | MNI Coordinates | | | BSR |
|---|---|---|---|---|---|---|---|---|---|
| | x | y | z | | | x | y | z | |
| **TR 1** | | | | | **TR 5 (cont)** | | | | |
| L. Precentral Gyrus | −20 | −7 | 48 | 5.092 | L. MTG | −61 | −51 | 3 | 4.186 |
| R. Middle Frontal Gyrus | 17 | 20 | 41 | 4.946 | R. Genu of Corpus Callosum | 24 | 37 | 3 | 4.178 |
| L. Middle Frontal Gyrus | −17 | 20 | 48 | 4.528 | L. Middle Frontal Gyrus | −44 | 54 | 3 | 4.073 |
| L. Middle Cingulate | 0 | −3 | 37 | 4.493 | L. Thalamus | −10 | −3 | 0 | 4.063 |
| R. Caudate Nucleus | 24 | 27 | 7 | 4.243 | Cerebellum | 3 | −51 | 3 | 4.059 |
| L. Inferior Occipital Gyrus | −41 | −75 | −7 | 3.814 | Cerebellum | 3 | −82 | −17 | 3.981 |
| L. Thalamus | −17 | −7 | 7 | 3.745 | L. Caudate Nucleus | −20 | 27 | 3 | 3.894 |
| L. Fusiform Gyrus | −41 | −48 | −3 | 3.514 | L. Middle Frontal Gyrus | −44 | 31 | 31 | 3.825 |
| R. Frontal Eye Fields | 27 | 0 | 37 | 3.457 | L. Middle Orbital Gyrus | −27 | −48 | −20 | 3.784 |
| **TR 2** | | | | | L. Calcarine Gyrus | −24 | −58 | 10 | 3.578 |
| R. Middle Frontal Gyrus | 31 | 20 | 48 | 5.879 | L. Fusiform Gyrus | −41 | −41 | −10 | 3.577 |
| R. Superior Medial Gyrus | 7 | 31 | 44 | 5.198 | **TR 6** | | | | |
| R. Occipitofrontal Fasciculus | 24 | 0 | 27 | 5.131 | L. Calcarine Gyrus | −3 | −95 | 10 | 6.722 |
| L. Hippocampus | −24 | −41 | 7 | 4.934 | L. Insula | −37 | −24 | 27 | 6.355 |
| R. Lingual Gyrus | 14 | −85 | −14 | 3.735 | R. Caudate Nucleus | 24 | 0 | 27 | 6.315 |
| R. Hippocampus | 27 | −41 | 3 | 3.694 | R. Genu of Corpus Callosum | 20 | 37 | 3 | 6.006 |
| L. Striatum | −20 | 20 | 7 | 3.484 | L. Caudate Nucleus | −20 | 27 | 3 | 5.664 |
| **TR 3** | | | | | Fusiform Gyrus | −37 | −51 | −3 | 5.270 |
| L. Thalamus | −24 | −41 | 10 | 6.403 | L. Superior Occipital Gyrus | −10 | −82 | 44 | 4.914 |
| R. Parahippocampal ctx | 31 | −37 | −7 | 5.541 | R. Occipital ctx | 27 | −78 | 10 | 4.704 |
| R. Inferior Frontal Gyrus | 51 | 7 | 17 | 5.131 | R. Rolandic Operculum | 48 | 0 | 17 | 4.682 |
| L. Inferior Frontal Gyrus | −44 | 44 | −10 | 4.326 | R. Lingual Gyrus | 10 | −92 | −10 | 4.511 |
| R. Inferior Frontal Gyrus | 48 | 37 | 14 | 4.232 | L. Posterior Cingulate | 0 | −31 | 31 | 4.317 |
| **TR 4** | | | | | R. Intraparietal Sulcus | 31 | −58 | 34 | 4.193 |
| R. Rolandic Operculum | 41 | −3 | 14 | 7.976 | L. Middle Frontal Gyrus | −44 | 31 | 31 | 3.816 |
| L Inferior Frontal Gyrus | −41 | 44 | 14 | 7.227 | R. Inferior Frontal Gyrus | 48 | 48 | −10 | 3.538 |
| R. Cerebellum | 20 | −71 | −17 | 4.506 | Thalamus | 27 | −20 | 0 | 3.236 |
| L. Superior Parietal Lobule | −24 | −75 | 51 | 3.973 | R. Inferior Parietal Lobule | −34 | −51 | 51 | 3.085 |
| L. Cerebellum | −24 | −65 | −17 | 3.681 | **TR 7** | | | | |
| L. Superior Frontal Gyrus | −14 | 58 | 17 | 3.351 | L. Hippocampus | −20 | −41 | 7 | 6.446 |
| L. Precuneus | 0 | −58 | 51 | 3.262 | R. Hippocampus | 20 | −34 | 10 | 6.064 |
| **TR 5** | | | | | R. Caudate Nucleus | 24 | −14 | 24 | 5.731 |
| R. Middle Cingulate | 14 | 24 | 41 | 7.786 | R. Genu of Corpus Callosum | 24 | 37 | 7 | 4.930 |
| L. Fusiform Gyrus | −27 | −71 | −14 | 5.089 | L. Caudate Nucleus | −17 | −3 | 24 | 4.707 |
| L. Superior Occipital Gyrus | −14 | −78 | 44 | 4.969 | L. Genu of Corpus Callosum | −20 | 27 | 20 | 4.275 |
| R. Postcentral Gyrus | 20 | −37 | 61 | 4.847 | L. Superior Frontal Gyrus | −14 | 24 | 44 | 3.833 |

Note: All activations survived a threshold of $p < 0.003$ (BSR $\leq 3$) with a minimum cluster size of 20 contiguous voxels. TR = time to repetition, BSR = Bootstrap Ratio, L = Left, R = Right, MTG = Middle Temporal Gyrus.

**Table 3B**
Regions associated with low rates of discounting.

| Brain Region | MNI Coordinates | | | BSR |
|---|---|---|---|---|
| | x | y | z | |
| **TR 1** | | | | |
| R. Putamen | 31 | −3 | −7 | −4.019 |
| L. Mid Orbital Gyrus | −3 | 44 | −7 | −3.768 |
| **TR 2** | | | | |
| R. SupraMarginal Gyrus | 51 | −41 | 24 | −4.665 |
| L. Anterior Cingulate | −10 | 44 | 10 | −4.415 |
| L. Cerebellum | −20 | −58 | −20 | −3.138 |
| **TR 3** | | | | |
| L. Inferior Parietal Lobule | −54 | −34 | 51 | −4.615 |
| R. Precentral Gyrus | 51 | 0 | 51 | −4.394 |
| R. MTG | 61 | −54 | 7 | −3.899 |
| R. Cerebellum | 24 | −51 | −27 | −3.725 |
| **TR 4** | | | | |
| R. SMA | 17 | 7 | 68 | −4.903 |
| **TR 7** | | | | |
| R. MTG | 48 | −44 | 0 | −5.221 |
| L. Anterior Cingulate | −3 | 34 | 10 | −4.636 |
| L. Inferior Parietal Lobule | −61 | −48 | 41 | −4.010 |
| R. Superior Temporal Gyrus | 51 | −17 | 3 | −3.967 |
| R. Inferior Temporal Gyrus | 44 | −44 | −17 | −3.881 |
| L. MTG | −48 | −20 | −3 | −3.602 |

Note: All activations survived a threshold of $p < 0.003$ (BSR $\leq -3$) with a minimum cluster size of 20 contiguous voxels. TR = time to repetition, BSR = Bootstrap Ratio, L = Left, R = Right, MTG = Middle Temporal Gyrus.

with heightened levels of risky decision making among problematic gamblers compared to healthy controls (Wang et al., 2016). Likewise, regions of the default network associated with self-referential thinking, Theory of Mind, and empathy were observed to be active on a social decision making task that required subjects to judge the moral justification of social actions and behaviors (Reniers et al., 2012). The default network might therefore play a dual role during DD and SD by allowing us to anticipate the future (DD) or social (SD) consequences of our choices in the immediate here and now.

Lastly, DD and SD evoked a common pattern of neural activity in mesolimbic and prefrontal regions involved with reward valuation (Montague et al., 2006) including the ventral striatum, lateral orbitofrontal cortex, and VMPFC. Valuation signals attached to appetitive, monetary, and social outcomes and stimuli evoke overlapping responses in these areas suggesting a common neural currency guiding choices across multiple domains (Levy and Glimcher, 2012; Montague et al., 2006). Overlap in these reward processing regions thus suggests that DD and SD each draw on common reward processing mechanisms when assigning value to competing intertemporal and interpersonal choice options.

### 4.2. Regions of DD-SD dissociation

We also observed patterns of brain activity that distinguished between the two discounting tasks. Neural dissociation was particularly

evident during the SD task, which was preferentially associated with activity in several default network regions. Intrinsic and task-based connectivity analyses have revealed distinct default network subsystems, each supporting unique components of abstract conceptual and associative processes (Andrews-Hanna et al., 2010; Andrews-Hanna et al., 2014a, b). Compared to DD, the SD task was associated with increased activity in the dorsomedial prefrontal cortex and bilateral TPJ. These regions are speculated to comprise a *mentalizing* default network subsystem involved with reflecting on the mental states of oneself and others. A recent study revealed consistent activation of the default network when mentalizing across a range of known others (including romantic partners, parents, close friends, and acquaintances) (Laurita et al., 2017). We also observed greater activity in anterior prefrontal and posterior cingulate cortices in response to the SD task. These regions are highly interconnected integration hubs within the default network and are active during tasks that require appraising the personal salience and affective impact of autobiographical stimuli (Andrews-Hanna et al., 2010; Buckner et al., 2008). This particular pattern of results may reflect the integration of prosocial considerations and personal preferences in support of strategic social behavior and decision making (Spreng and Mar, 2011).

In the present study, participants made similar financial decisions involving variable temporal and social distances. One limitation of this design is that financial decisions involving social beneficiaries may elicit ambiguous economic and psychological considerations. For example, an undergraduate student may elect to take the smaller selfish outcome in favor of allocating $100 to a socially close but financially well-off parent. We attempted to limit this potential confound by avoiding choices involving financial benefactors (e.g., parents, grandparents). Another possibility is that selecting the altruistic option for socially proximal beneficiaries often entails immediate personal benefits (e.g., shared bank account with a significant other). In such cases, a decision maker may bypass consideration of social distance when assigning value to social outcomes that entail immediate personal benefits. Though we cannot completely rule out this possibility, engagement of the default network mentalizing subsystem supports our hypothesis that social considerations influence preferences on the SD task. Future studies may wish to incorporate control trials designed to isolate temporal and social projection while holding the financial decision constant (e.g., $100 in 1 month vs. $100 in 6 months; $100 for person 2 vs. $100 for person 8) in order to clarify the brain regions encoding temporal and social distance and their influence on behavioral preferences.

A second limitation is that financial decisions in both temporal and social paradigms may minimize the differences between the processes. Future studies may wish to use non-monetary altruistic choices to assess a more distinct type of decision. Likewise, given prior observations of qualitative differences between DD and SD, future studies that vary choice dimensions such as reward magnitudes and motivational valence (i.e., gains vs. losses) may elucidate additional neural differences between the two forms of discounting.

### 4.3. Neural correlates of behavioral heterogeneity in discount rates

We also observed a pattern of brain activity that differentiated between high and low discounters. Across both conditions, higher rates of discounting (i.e., impulsive and/or selfish individuals) were associated with increased MTL and fronto-insular activity. Similar neural patterns were observed in a recent study that asked smokers to view pictures of environments associated with their personal smoking behavior (McClernon et al., 2016). Compared to viewing nonsmoking environments and proximal smoking cues (e.g., lit cigarette), viewing personal smoking environments led to increased posterior hippocampal and insular activity. Activity in the right anterior insula in response to viewing personal smoking environments was correlated with subsequent ad libitum smoking behavior after a 6 h period of abstinence. These results may reflect a biological mechanism of drug-environment associations (McClernon et al., 2016). In a study of adolescent substance abusers, higher rates of DD were associated with greater activity in a distributed network of limbic and paralimbic regions, including the hippocampus and insular cortex (Stanger et al., 2013) and hippocampal and parahippocampal white matter volume has been observed to positively correlate with rates of DD (Yu, 2012). Likewise, parametric modulation of right hippocampus and insula by selfish reward magnitudes was previously observed during SD trials in which participant selected the smaller selfish option (Strombach et al., 2015; Table S1). Our observation of increased MTL and fronto-insular activity among high discounters is consistent with a bottom-up reward valuation account wherein limbic structures place greater weight on the affective impact of immediate gratification (McClure et al., 2004; Stanger et al., 2013).

Our observation of increased MTL activity among high discounters draws attention to contradictory reports of hippocampal functioning during intertemporal decision making. The predominant account of MTL involvement in discounting is that the hippocampus supports deliberative, flexible cognition by allowing us to modify and update knowledge representations with new information, which in turn can help inform and optimize choices involving uncertain future or social outcomes (Palombo, Keane and Verfaellie, 2015a; Reddish, 2016; Rubin et al., 2014; Spreng, 2013; Wang et al., 2014; Yu and Frank, 2015). Rats with hippocampal lesions tend to prefer small immediate rewards over larger time-delayed rewards (Mariano et al., 2009; McHugh et al., 2008) and in humans hippocampal volume is positively correlated with behavioral inhibition (Cherbuin et al., 2008).

However, amnesic patients with bilateral MTL damage exhibit relatively normal rates of DD despite an inability to anticipate future outcomes (Kwan et al., 2012; Palombo, Keane and Verfaelli, 2015b). Hippocampal mediated deliberative foresight is therefore not a necessary precondition for choosing between competing intertemporal options but instead might reflect a neurobehavioral mechanism by which time-delayed reward signals are adaptively modulated in order to sway choice preferences (Benoit et al., 2011; Boyer, 2008; Bulley et al., 2016; Kwan et al., 2015; Peters and Buchel, 2010). The conditions in which hippocampal activity is associated with bottom-up valuation (as we observed) or top-down deliberation will be a worthwhile topic of follow up investigation.

The behavioral PLS also revealed a pattern of increased medial prefrontal and right TPJ activity among low discounters in both conditions (i.e., more self-controlled and/or altruistic individuals). The right TPJ is putatively regarded as supporting social cognitive processes, such as self-other distinctions (Hartwright et al., 2014; Saxe et al., 2004) and simulating mental states (Spreng et al., 2009). This region was previously observed to functionally couple with the VMPFC during generous, but not selfish, choices on a SD task, potentially reflecting the modulation of valuation signals by superordinate, prosocial considerations (Strombach et al., 2015). Our findings in these regions therefore largely corroborate the presumed functional role of TPJ activity on a SD task and also highlight a potential analogous role in response to far-sighted preferences on a DD task. Though not part of a core DD network (Carter et al., 2010), activity in the right TPJ is observed during intertemporal choices that place greater demands on extracting information about future affective states (O'Connell et al., 2015). Moreover, transcranial magnetic inhibition of the right TPJ was recently observed to produce steeper rates of discounting for both delayed and social rewards, potentially reflecting a common neurocognitive mechanism facilitating self-controlled and altruistic choices (Soutschek et al., 2016).

We also observed greater VMPFC activity among low discounters which we believe may reflect processes involved with mentally simulating the affective impact of delayed or social outcomes (Boyer, 2008). Economic models of intertemporal choice have often treated the decision making agent as a single entity across time. However, increasing evidence indicates that intertemporal choices might be more aptly characterized as conflicts between allocating resources between one's present-self and a psychologically distinct future-self (Ersner-Hershfield

et al., 2009; Mitchell et al., 2011; Simon, 1995). Perceived overlap or continuity between one's current and future selves (indexed by less VMPFC *deactivation* when making trait judgments about oneself in the future) is predictive of lower delay discounting (Ersner-Hershfield et al., 2009; Mitchell et al., 2011). Similar results are observed in the social domain. For example, activity in the VMPFC in response to a mentalizing task is parametrically modulated by perceived self-other similarity (Benoit et al., 2010; Mitchell, Banaji, & Macrae, 2005) and less VMPFC *deactivation* is predictive of optimal performance on a social reasoning task (Coricelli and Nagel, 2009). The ability to vividly simulate episodic imagery corresponding to future or social outcomes has been observed to reduce rates of DD (Benoit et al., 2011; Hakimi and Hare, 2015; Peters and Buchel, 2010) and SD (Yi et al., 2016) and facilitate prosocial intentions (Gaesser and Schacter, 2014). Taken together, we suggest that higher rates of intertemporal self-control and interpersonal altruism place similar demands on simulating mental states mediated by VMPFC and right TPJ activity – the mental state of oneself in the future (DD) or the mental state of the beneficiary of one's generosity (SD) (see also Soutschek et al., 2016).

Behavioral DD and SD choice indices were not correlated, potentially due to our relatively smaller sample size. However, the lack of correlation between behavioral discount rates does not conflict with the behavioral PLS results that identified common patterns of brain activity differentiating between high and low discounters across both tasks. Critically, the behavioral PLS revealed common brain regions that independently covaried with DD and SD choice indices at the group level but were free to vary at the individual level. Thus, individual differences in the brain-behavior relationships were independent of within-subject behavioral DD-SD correlations. For example, a high DD (impulsive) but low SD (altruistic) individual would be characterized by greater MTL and limbic activity during the DD task (corresponding to lower intertemporal self-control) but greater VMPFC and TPJ activity during the SD task (corresponding to higher interpersonal altruism). In contrast, an individual that scored low on both discount measures (i.e., self-controlled and altruistic) would be expected to similarly engage VMPFC and TPJ regions in response to both discounting tasks. These results suggest that, although DD and SD engage similar neural networks, within-subject recruitment of these regions might be motivated by different underlying factors. This will be a promising direction for identifying potential behavioral and/or neural divergence between DD and SD.

It is also worth noting that a key piece of evidence for functional overlap between DD and SD is the behavioral finding that both forms of discounting are well characterized as a hyperbolic function of increasing temporal or social distance. The paradigm used in this study prevented a robust estimation of hyperbolic discount rates. Future studies may wish to address this by incorporating alternative methods to obtain both model-based and model-free discount parameters. Likewise, our sample was predominantly female (18 female, 7 male) and consisted of graduate and undergraduate students. On re-analysis of the data, we separated our participants by sex and found no significant sex interaction. However, future studies may wish to obtain more representative samples in order to account for potential SES and sex differences on financial and/or social preferences (Croson and Gneezy, 2009; Kamas and Preston, 2015; cf. Cross et al., 2011).

### 4.4. Conclusions

Researchers have identified a close functional correspondence between decision making processes that support choices involving future and other-regarding outcomes but the relationship between this behavioral correspondence and underlying neural networks has not been established. We observed extensive neural congruence between DD and SD indicating a common functional and neuroanatomical basis of decisions that require the construction of alternative perspectives (Buckner and Carroll, 2007) across dimensions of temporal and interpersonal distance. These results thus build on prior behavioral and theoretical work emphasizing a close functional link between behavioral self-control and social altruism. We also observed a common pattern of brain activity distinguishing between high and low discounters in regions involved with bottom-up valuation and mental simulation, respectively. These results thus offer a potential biological mechanism underlying behavioral heterogeneity in discount rates across both forms of discounting. In addition to the extensive neural overlap, we also observed patterns of neural activity that distinguished between the two discounting conditions. SD trials were associated with increased activity in default network regions involved with self-appraisal and mentalizing. Taken together, these results are particularly crucial in light of the psychosocial ramifications of behaviors associated with excessive temporal discounting and growing evidence for the influence of social context on reinforcer valuation and increased self-control (Bickel et al., 2012a, b; Charlton et al., 2013; Kishida and Montague, 2012). Ultimately, a greater understanding of the common and unique neurocognitive basis of these two modes of decision making will shed light on the factors underlying normative and maladaptive decision making and provide valuable insights into potential approaches and phenotypic targets for engendering behavioral change across disparate forms of temporal and social impulsivity.

## Acknowledgments

The authors wish to thank Amber Koch, Samantha Boothe, and Cynthia Guerin for their assistance with data collection and analysis. Funding for this project was provided by National Institutes of Health grant MH083945.

## Appendix A. Supplementary data

Supplementary data related to this article can be found at http://dx.doi.org/10.1016/j.neuroimage.2017.08.071.

## References

Andrews-Hanna, J.R., Reidler, J.S., Sepulcre, J., Poulin, R.L., 2010. Functional-anatomic fractionation of the brain's default network. Neuron 65, 550–562. http://dx.doi.org/10.1016/j.neuron.2010.02.005.

Andrews-Hanna, J.R., Saxe, R., Yarkoni, T., 2014a. Contributions of episodic retrieval and mentalizing to autobiographical thought: evidence from functional neuroimaging, resting-state connectivity, and fMRI meta-analyses. NeuroImage 91, 324–335. http://dx.doi.org/10.1016/j.neuroimage.2014.01.032.

Andrews-Hanna, J.R., Smallwood, J., Spreng, R.N., 2014b. The default network and self-generated thought: component processes, dynamic control, and clinical relevance. Ann. N. Y. Acad. Sci. 1316, 29–52. http://dx.doi.org/10.1111/nyas.12360.

Atanasov, P.D., 2016. Risk Preferences in Choices for Self and Others: Meta-Analysis and Research Directions. http://dx.doi.org/10.2139/ssrn.1682569. Available at: SSRN.

Axelrod, R., Hamilton, W.D., 1981. The evolution of cooperation. Science 211, 1390–1396.

Bechara, A., Damasio, H., Tranel, D., Damasio, A.R., 2005. The Iowa Gambling Task and the somatic marker hypothesis: some questions and answers. Trends Cognit. Sci. 9 (4), 159–162. http://dx.doi.org/10.1016/j.tics.2005.02.002.

Benoit, R.G., Gilbert, S.J., Burgess, P.W., 2011. A neural mechanism mediating the impact of episodic prospection on farsighted decisions, 31 (18), 6771–6779. http://dx.doi.org/10.1523/JNEUROSCI.6559-10.2011.

Benoit, R.G., Gilbert, S.J., Volle, E., Burgess, P.W., 2010. When I think about me and simulate you: medial rostral prefrontal cortex and self-referential processes. NeuroImage 50 (3), 1340–1349. http://dx.doi.org/10.1016/j.neuroimage.2009.12.091.

Bickel, W.K., Jarmolowicz, D.P., Mueller, T., Franck, C.T., Carrin, C., Gatchalian, K.M., 2012a. Altruism in time: social temporal discounting differentiates smokers from problem drinkers. Psychopharmacology 224, 109–120. http://dx.doi.org/10.1007/s00213-012-2745-6.

Bickel, W.K., Jarmolowicz, D.P., Mueller, T., Koffarnus, M.N., Gatchalian, K.M., 2012b. Excessive discounting of delayed reinforcers as a trans-disease process contributing to addiction and other disease-related vulnerabilities: emerging evidence. Pharmacol. Ther. 134, 287–297. http://dx.doi.org/10.1016/j.pharmthera.2012.02.004.

Bickel, W.K., Pitcock, J.A., Yi, R., Angtuaco, E.J.C., 2009. Congruence of BOLD response across intertemporal choice conditions: fictive and real money gains and losses, 29 (27), 8839–8846. http://dx.doi.org/10.1523/JNEUROSCI.5319-08.2009.

Boettiger, C.A., Mitchell, J.M., Tavares, V.C., Robertson, M., Joslyn, G., Esposito, M.D., Fields, H.L., 2007. Immediate reward bias in humans: fronto-parietal networks and a role for the catechol-O-methyltransferase 158 val/val genotype. J. Neurosci. 27 (52), 14383–14391. http://dx.doi.org/10.1523/JNEUROSCI.2551-07.2007.

Boyer, P., 2008. Evolutionary economics of mental time travel. Trends Cognit.Sci. 12 (6), 219–224. http://dx.doi.org/10.1016/j.tics.2008.03.003.
Buckner, R.L., Andrews-Hanna, J.R., Schacter, D.L., 2008. The brain's default network: anatomy, function, and relevance to disease. The Year in Cognit.Neuroscience –Annals of the NY Academy of Sci, 1124, 1–38.
Buckner, R.L., Carroll, D.C., 2007. Self-projection and the brain. Trends Cognit.Sci. 11 (2), 49–57. http://dx.doi.org/10.1016/j.tics.2006.11.004.
Bulley, A., Henry, J., Suddendorf, T., 2016. Prospection and the present moment: the role of episodic foresight in intertemporal choices between immediate and delayed rewards. Rev. General Psychol. 20 (1), 29–47. http://dx.doi.org/10.1037/gpr0000061.
Burrow, A.L., Spreng, R.N., 2016. Waiting with purpose: a reliable but small association between purpose in life and impulsivity. Pers. Individ. Differ. 90, 187–189.
Carter, R.M., Meyer, J.R., Huettel, S.A., 2010. Functional neuroimaging of intertemporal choice models: a review, 3 (1), 27–45. http://dx.doi.org/10.1037/a0018046.
Charlton, S.R., Yi, R., Porter, C., Carter, A., Bickel, W., Rachlin, H., 2013. Now for me, later for us? Effects of group context on temporal discounting. J. Behab Decis. Mak. 26 (2), 118–127. http://dx.doi.org/10.1002/bdm.766.
Cherbuin, N., Windsor, T.D., Anstey, K.J., Maller, J.J., Meslin, C., Sachdev, P.S., 2008. Hippocampal volume is positively associated with behavioural inhibition (BIS) in a large community-based sample of mid-life adults: the PATH through life study. Soc. Cognit.Affect. Neurosci. 3 (3), 262–269. http://dx.doi.org/10.1093/scan/nsn018.
Coricelli, G., Nagel, R., 2009. Neural correlates of depth of strategic reasoning in medial prefrontal cortex. PNAS 106 (23), 1–6.
Croson, R., Gneezy, U., 2009. Gender differences in preferences. J. Econ. Lit. 47 (2), 448–474. http://dx.doi.org/10.1257/jel.47.2.448.
Cross, C.P., Copping, L.T., Campbell, A., 2011. Sex differences in Impulsivity : a meta-analysis. Psychol. Bull. 137 (1), 97–130. http://dx.doi.org/10.1037/a0021591.
Ersner-Hershfield, H., Wimmer, G.E., Knutson, B., 2009. Saving for the future self: neural measures of future self-continuity predict temporal discounting. Soc. Cognit.Affect. Neurosci. 4 (1), 85–92. http://dx.doi.org/10.1093/scan/nsn042.
Friston, K.J., Penny, W.D., Glaser, D.E., 2005. Conjunction revisited. NeuroImage 25, 661–667. http://dx.doi.org/10.1016/j.neuroimage.2005.01.013.
Gaesser, B., Schacter, D.L., 2014. Episodic simulation and episodic memory can increase intentions to help others. Proc. Natl. Acad. Sci. U. S. A. 111 (12), 4415–4420. http://dx.doi.org/10.1073/pnas.1402461111.
Gerlach, K.D., Spreng, R.N., Gilmore, A.W., Schacter, D.L., 2011. Solving future problems: default network and executive activity associated with goal-directed mental simulations. NeuroImage 55 (4), 1816–1824. http://dx.doi.org/10.1016/j.neuroimage.2011.01.030.
Gerlach, K.D., Spreng, R.N., Madore, K.P., Schacter, D.L., 2013. Future planning: default network activity couples with frontoparietal control network and reward-processing regions during process and outcome simulations. Soc. Cognit. Affect. Neurosci. 9 (12), 1942–1951. http://dx.doi.org/10.1093/scan/nsu001.
Green, L., Myerson, J., 2004. A discounting framework for choice with delayed and probabilistic rewards. Psychol. Bull. 130, 769–792.
Hakimi, X.S., Hare, X.T.A., 2015. Enhanced neural responses to imagined primary rewards predict reduced monetary temporal discounting, 35 (38), 13103–13109. http://dx.doi.org/10.1523/JNEUROSCI.1863-15.2015.
Harris, A.C., Madden, G.J., 2002. Delay discounting and performance on the prisoner's dilemma game. Psychol. Rec. 52, 429–440.
Hartwright, C.E., Apperly, I.A., Hansen, P.C., 2014. Representation, control, or reasoning? Distinct functions for theory of mind within the medial prefrontal cortex. J. Cogn. Neurosci. 26, 683–698. http://dx.doi.org/10.1162/jocn_a_00520.
Jimura, K., Chushak, M.S., Braver, T.S., 2013. Impulsivity and self-control during intertemporal decision making linked to the neural dynamics of reward value representation, 33 (1), 344–357. http://dx.doi.org/10.1523/JNEUROSCI.0919-12.2013.
Jones, B., Rachlin, H., 2006. Social discounting. Psychol. Sci. 17 (4), 283–286.
Jones, B.A., Rachlin, H., 2009. Delay, probability, and social discounting in a public goods game. J. Exp. Anal. Behav. 91, 61–73. http://dx.doi.org/10.1901/jeab.2009.91-61.
Kable, J.W., Glimcher, P.W., 2007. The neural correlates of subjective value during intertemporal choice. Nat. Neurosci. 10 (12), 1625–1634. http://dx.doi.org/10.1038/nn2007.
Kamas, L., Preston, A., 2015. Journal of Economic Behavior & Organization Can social preferences explain gender differences in economic behavior ? J. Econ. Behav. Organ. 116, 525–539. http://dx.doi.org/10.1016/j.jebo.2015.05.017.
Kishida, K.T., Montague, P.R., 2012. Imaging models of valuation during social interaction in humans. BPS 72 (2), 93–100. http://dx.doi.org/10.1016/j.biopsych.2012.02.037.
Kwan, D., Craver, C.F., Green, L., Myerson, J., Boyer, P., Rosenbaum, R.S., 2012. Future decision-making without episodic mental time travel. Hippocampus 22 (6), 1215–1219. http://dx.doi.org/10.1002/hipo.20981.
Kwan, D., Craver, C.F., Green, L., Myerson, J., Gao, F., Black, S.E., Rosenbaum, R.S., 2015. Cueing the personal future to reduce discounting in intertemporal choice: is episodic prospection necessary? Hippocampus 25 (4), 432–443. http://dx.doi.org/10.1002/hipo.22431.
Laurita, A.C., Hazan, C., Spreng, R.N., 2017. Dissociable patterns of brain activity for mentalizing about known others: a role for attachment. Soc. Cognit. Affect. Neurosci. http://dx.doi.org/10.1093/scan/nsx040. Advance online publication.
Levy, D.J., Glimcher, P.W., 2012. The root of all value: a neural common currency for choice. Curr. Opin. Neurobiol. 22 (6), 1027–1038. http://dx.doi.org/10.1016/j.conb.2012.06.001.
Locey, M.L., Jones, B.A., Rachlin, H., 2011. Real and hypothetical rewards in social discounting. Judgm. Decis. Mak. 6 (6), 552–564.
Mariano, T.Y., Bannerman, D.M., McHugh, S.B., Preston, T.J., Rudebeck, P.H., Rudebeck, S.R., Campbell, T.G., 2009. Impulsive choice in hippocampal but not orbitofrontal cortex-lesioned rats on a nonspatial decision-making maze task. Eur. J. Neurosci. 30 (3), 472–484. http://dx.doi.org/10.1111/j.1460-9568.2009.06837.x.
McClernon, F.J., Conklin, C.A., Kozink, R.V., Adcock, R.A., Sweitzer, M.M., Addicott, M.A., Devito, A.M., 2016. Hippocampal and insular response to smoking-related Environments . Neuroimaging Evid. Drug Context Eff. Nicotine Depend. 41 (3), 877–885. http://dx.doi.org/10.1038/npp.2015.214.
McClure, S.M., Bickel, W.K., 2014. A dual-systems perspective on addiction: contributions from neuroimaging and Cognit.training. Ann. N. Y. Acad. Sci. 1327, 62–78. http://dx.doi.org/10.1111/nyas.12561.
McClure, S.M., Laibson, D.I., Loewenstein, Cohen, J.D., 2004. Separate neural systems value immediate and delayed monetary rewards. Science 306, 503–507. http://dx.doi.org/10.1126/science.1100907.
McHugh, S.B., Campbell, T.G., Taylor, A.M., Rawlins, J.N.P., Bannerman, D.M., 2008. A Role for Dorsal and Ventral Hippocampus in Inter-Temporal Choice Cost-Benefit Decision Making. http://dx.doi.org/10.1037/0735-7044.122.1.1.
McIntosh, A.R., Lobaugh, N.J., 2004. Partial least squares analysis of neuroimaging data: applications and advances. NeuroImage 23, 250–263. http://dx.doi.org/10.1016/j.neuroimage.2004.07.020.
Mitchell, J.P., Banaji, M.R., Macrae, C.N., 2005. The link between social cognition and self-referential thought in the medial prefrontal cortex. J. Cognit. Neurosci. 17 (8), 1306–1315. http://dx.doi.org/10.1162/0898929055002418.
Mitchell, J.M., Fields, H.L., D'Esposito, M., Boettiger, C.A., 2005. Impulsive responding in alcoholics. Alcohol. Clin. Exp. Res. 29 (12), 2158–2169, 0000374-200512000-00010 [pii].
Mitchell, J.P., Schirmer, J., Ames, D.L., Gilbert, D.T., 2011. Medial prefrontal cortex predicts intertemporal choice. J. Cognit. Neurosci. 23 (4), 857–866. http://dx.doi.org/10.1162/jocn.2010.21479.
Moffitt, T.E., Arseneault, L., Belsky, D., Dickson, N., Hancox, R.J., Harrington, H., Caspi, A., 2011. A gradient of childhood self-control predicts health, wealth, and public safety. Proc. Nat. Acad. Sci. U. S.A. 108 (7), 2693–2698. http://dx.doi.org/10.1073/pnas.1010076108.
Montague, P.R., King-Casas, B., Cohen, J.D., 2006. Imaging valuation models in human, choice. Annu. Rev. Neurosci. 29, 417–448. http://dx.doi.org/10.1146/annurev.neuro.29.051605.112903.
O'Connell, G., Christakou, A., Chakrabarti, B., 2015. The role of simulation in intertemporal choices. Front. Neurosci. 9, 1–10. http://dx.doi.org/10.3389/fnins.2015.00094. MAR.
Odum, A.L., 2011. Delay discounting: I'm a k, you're a k. J. Exp. Anal. Behav. 96, 427–439. http://dx.doi.org/10.1901/jeab.2011.96-423.
Palombo, D.J., Keane, M.M., Verfaellie, M., 2015a. How does the hippocampus shape decisions? Neurobiol. Learn. Mem. 125, 93–97. http://dx.doi.org/10.1016/j.nlm.2015.08.005.
Palombo, D.J., Keane, M.M., Verfaellie, M., 2015b. The medial temporal lobes are critical for reward-based decision making under conditions that promote episodic future thinking. Hippocampus 25 (3), 345–353. http://dx.doi.org/10.1002/hipo.22376.
Peters, J., Buchel, C., 2010. Episodic future thinking reduces reward delay discounting through an enhancement of prefrontal-mediotemporal interactions. Neuron 66, 138–148. http://dx.doi.org/10.1016/j.neuron.2010.03.026.
Peters, J., Buchel, C., 2011. The neural mechanisms of understanding variability. Trends Cogn. Sci. 15 (5), 227–239. http://dx.doi.org/10.1016/j.tics.2011.03.002.
Price, C.J., Friston, K.J., 1997. Cognitive conjunction : a new approach to brain activation experiments, 270 (5), 261–270.
Rachlin, H., 2002. Altruism and selfishness. Behav. Brain Sci. 25, 239–296.
Rachlin, H., Jones, B.A., 2007. Social discounting and delay discounting. J. Behav. Decis. Mak. 21, 29–43. http://dx.doi.org/10.1002/bdm.567.
Reddish, A.D., 2016. Vicarious trial and error. Nat. Rev. Neurosci. 17, 147–159. http://dx.doi.org/10.1038/nrn.2015.30.
Reniers, R.L.E.P., Corcoran, R., Völlm, B.A., Mashru, A., Howard, R., Liddle, P.F., 2012. Moral decision-making, ToM, empathy and the default mode network. Biol. Psychol. 90 (3), 202–210. http://dx.doi.org/10.1016/j.biopsycho.2012.03.009.
Rilling, J.K., Sanfey, A.G., 2011. The neuroscience of social decision-making. Annu. Rev. Psychol. 62, 23–48. http://dx.doi.org/10.1146/annurev.psych.121208.131647.
RStudio Team, 2015. RStudio: Integrated Development for R. RStudio, Inc., Boston, MA. URL http://www.rstudio.com/.
Rubin, R.D., Watson, P.D., Duff, M.C., Cohen, N.J., 2014. The role of the hippocampus in flexible cognition and social behavior. Front. Hum. Neurosci. 8, 1–15. http://dx.doi.org/10.3389/fnhum.2014.00742. September.
Safin, V., Locey, M.L., Rachlin, H., 2013. Valuing rewards to others in a prisoner's dilemma game. Behav. Process. 99, 145–149. http://dx.doi.org/10.1016/j.beproc.2013.07.008.
Saxe, R., Carey, S., Kanwisher, N., 2004. Understanding other minds: linking developmental psychology and functional neuroimaging. Annu. Rev. Psychol. 55, 87–124. http://dx.doi.org/10.1146/annurev.psych.55.090902.142044.
Shamosh, N.A., DeYoung, C.G., Green, A.E., Reis, D.L., Johnson, M.R., Conway, A.R., Gray, J.R., 2008. Individual differences in delay discounting: Relation to intelligence, working memory, and anterior prefrontal cortex. Psychol. Sci. 19, 904–911. http://dx.doi.org/10.1111/j.1467-9280.2008.02175.x.
Simon, J., 1995. Interpersonal allocation continuous with intertemporal allocation. Ration. Soc. 7, 367–392.
Soutschek, A., Ruff, C.C., Strombach, T., Kalenscher, T., Tobler, P.N., 2016. Brain stimulation reveals crucial role of overcoming self-centeredness in self-control. Sci. Adv. 2 (10) http://dx.doi.org/10.1126/sciadv.1600992 e1600992.
Spreng, R.N., 2013. Examining the role of memory in social cognition. Front. Psychol. 4 (July), 2012–2013. http://dx.doi.org/10.1037/a0029869.

Spreng, R.N., Gerlach, K.D., Turner, G.R., Schacter, D.L., 2015. Autobiographical planning and the brain: activation and its modulation by qualitative features. J. Cognit. Neurosci. 27, 2147–2157.

Spreng, R.N., Mar, R.A., 2011. I remember you : a role for memory in social cognition and the functional neuroanatomy of their interaction. Brain Res. http://dx.doi.org/10.1016/j.brainres.2010.12.024.

Spreng, R.N., Mar, R.A., Kim, A.S.N., 2009. The common neural basis of autobiographical memory, prospection, navigation, theory of mind, and the default mode: a quantitative meta-analysis. J. Cognit. Neurosci. 21 (3), 489–510. http://dx.doi.org/10.1162/jocn.2008.21029.

Spreng, R.N., Stevens, W.D., Chamberlain, J.P., Gilmore, A.W., Schacter, D.L., 2010. Default network activity, coupled with the frontoparietal control network, supports goal-directed cognition. NeuroImage 53 (1), 303–317. http://dx.doi.org/10.1016/j.neuroimage.2010.06.016.

Sridharan, D., Levitin, D.J., Menon, V., 2008. A critical role for the right fronto-insular cortex in switching between central-executive and default-mode networks. Proc. Natl. Acad. Sci. U. S. A. 105 (34), 12569–12574. http://dx.doi.org/10.1073/pnas.0800005105.

Stanger, C., Elton, A., Ryan, S.R., James, G.A., Budney, A.J., Kilts, C.D., 2013. Neuroeconomics and adolescent substance abuse: individual differences in neural networks and delay discounting. J. Am. Acad. Child Adolesc. Psychiatry 52 (7), 747–755. http://dx.doi.org/10.1016/j.jaac.2013.04.013 e6.

Stephens, D.W., McLinn, C.M., Stevens, J.R., 2002. Discounting and reciprocity in an iterated prisoner's dilemma. Science 298, 2216–2218.

Strombach, T., Weber, B., Hangebrauk, Z., Kenning, P., Karipidis, I.I., Tobler, P.N., 2015. Social discounting involves modulation of neural value signals by temporoparietal junction. Proc. Nat. Acad. Sci. U. S. A. 112 (5), 1619–1624. http://dx.doi.org/10.1073/pnas.1414715112.

Trope, Y., Liberman, N., 2010. Constual-level theory of psychological distance. Psychol. Rev. 117 (2), 440–463. http://dx.doi.org/10.1037/a0018963.

Vincent, J.L., Kahn, I., Snyder, A.Z., Raichle, M.E., Buckner, R.L., 2008. Evidence for a frontoparietal control system revealed by intrinsic functional connectivity. J. Neurophysiol. 100 (6), 3328–3342. http://dx.doi.org/10.1152/jn.90355.2008.

Wang, J.X., Cohen, N.J., Voss, J.L., 2014. Covert rapid action-memory simulation (CRAMS): a hypothesis of hippocampal-prefrontal interactions for adaptive behavior. Neurobiol. Learn. Mem. 117, 22–33. http://dx.doi.org/10.1016/j.nlm.2014.04.003.

Wang, L., Wu, L., Lin, X., Zhang, Y., Zhou, H., Du, X., Dong, G., 2016. Dysfunctional default mode network and executive control network in people with Internet gaming disorder: independent component analysis under a probability discounting task. Eur. Psychiatry 34, 36–42. http://dx.doi.org/10.1016/j.eurpsy.2016.01.2424.

Warton, D.I., Hui, K.C., 2011. The arcsine is asinine: the analysis of proportions in ecology. Ecology 92 (1), 3–10. http://dx.doi.org/10.1890/10-0340.1.

Yi, R., Carter, A.E., Landes, R.D., 2012. Restricted psychological horizon in active methamphetamine users: future, past, probability, and social discounting. Behav. Pharmacol. 23 (4), 358–366. http://dx.doi.org/10.1097/FBP.0b013e3283564e11.

Yi, R., Charlton, S., Porter, C., Carter, A.E., Bickel, W.K., 2011. Future altruism: social discounting of delayed rewards. Behav. Process. 86 (1), 160–163. http://dx.doi.org/10.1016/j.beproc.2010.09.003.

Yi, R., Johnson, M.W., Bickel, W.K., 2005. Relationship between cooperation in an iterated prisoner's dilemma game and the discounting of hypothetical outcomes. Learn. Behav. 33, 324–336.

Yi, R., Pickover, A., Stuppy-Sullivan, A.M., Baker, S., Landes, R.D., 2016. Impact of episodic thinking on altruism. J. Exp. Soc. Psychol. 65, 74–81. http://dx.doi.org/10.1016/j.jesp.2016.03.005.

Yu, R., 2012. Regional white matter volumes correlate with delay discounting. PLoS ONE 7 (2). http://dx.doi.org/10.1371/journal.pone.0032595.

Yu, J.Y., Frank, L.M., 2015. Hippocampal-cortical interaction in decision making. Neurobiol. Learn. Mem. 117, 34–41. http://dx.doi.org/10.1016/j.nlm.2014.02.002.